Processing Stability of Monolayer WS_2 on SiO_2

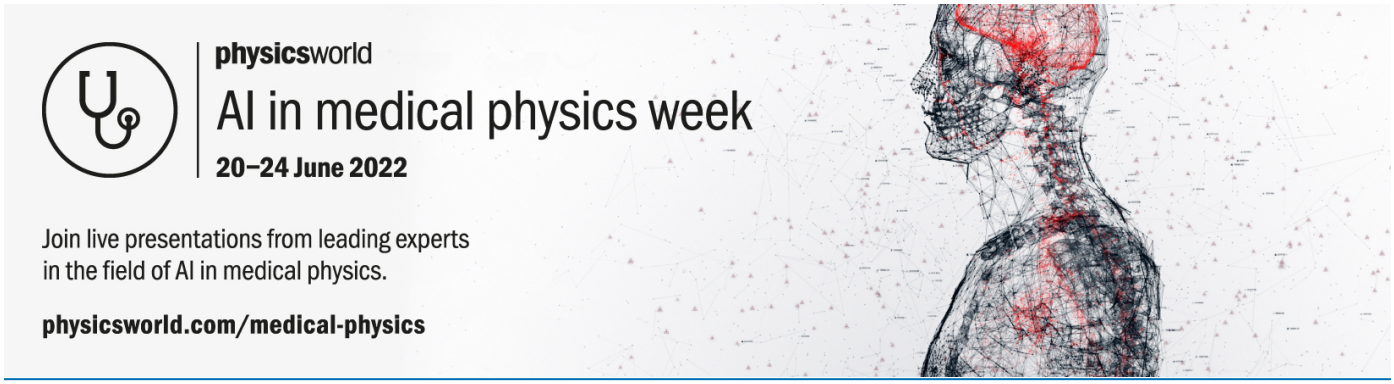

NANO EXPRESS

PAPER

Processing Stability of Monolayer WS_2 on SiO_2

G Delie[1], D Chiappe[2,3], I Asselberghs[2], C Huyghebaert[2], I Radu[2], S Banerjee[2], B Groven[2], S Brems[2] and V V Afanas'ev[1]

[1] Department of Physics and Astronomy, University of Leuven, 3001 Leuven, Belgium
[2] Imec, Kapeldreef 75, 3001 Leuven, Belgium
[3] Present address: ASM Microchemistry, Pietari Kalmin katu 3, F 2, 00560 Helsinki, Finland

E-mail: gilles.delie@kuleuven.be

Keywords: internal photoemission, interface barrier, 2D semiconductor, band offset

OPEN ACCESS

RECEIVED
24 December 2020

REVISED
9 April 2021

ACCEPTED FOR PUBLICATION
4 May 2021

PUBLISHED
24 May 2021

Abstract

Using internal photoemission of electrons, the energy position of the valence band top edge in 1 monolayer WS_2 films on top of SiO_2 thermally-grown on Si was monitored to evaluate the stability of the WS_2 layer with respect to two critically important technological factors: exposure to air and the transfer of WS_2 from the growth substrate (sapphire) onto SiO_2. Contrary to previous results obtained for WS_2 and MoS_2 layers synthesized by metal film thermal sulfurization in H_2S, the valence band top of metal-organic chemical vapor deposition grown WS_2 is found to remain at 3.7 ± 0.1 eV below the conduction band bottom edge of SiO_2 through different growth runs, transfer processing, and storage in air for several months. This exceptional stability indicates WS_2 as a viable candidate for the wafer-scale technology implementation.

1. Introduction

Since the first demonstration of a functional single-monolayer (ML) MoS_2 metal-oxide-semiconductor transistor by Radisavljevic *et al* [1], transistors with two-dimensional (2D) transition metal dichalcogenide (TMD) channels have been extensively explored [2–4]. While this research initially was mainly focused on the stable and readily available MoS_2, single- and few-ML WS_2 layers might be more promising due to a higher electron mobility [5] and a better ON/OFF current ratio [6]. However, most of these experimental transistors are based on 2D layers obtained by exfoliation from a bulk crystal, which is incompatible with the wafer-scale processing commonly used to fabricate integrated circuits (IC). While the growth of large area 2D TMD layers is potentially achievable by various techniques [7–9] ranging from molecular beam epitaxy to the industry standard chemical vapor deposition (CVD) [10], numerous difficulties are encountered in terms of high sensitivity of the interface properties to the processing details. For example, the electron band alignment of 2D layers with oxide substrates, e.g. SiO_2, may vary by ≈ 0.5 eV for different synthesis methods of few-ML thin MoS_2 as revealed by the valence band (VB) top energy shift [11]. More recently we observed that the growth method affects the band alignment at the WS_2/SiO_2 interface though to a considerably lesser extent than in the case of MoS_2/SiO_2 structures [12]. Furthermore, not only the TMD synthesis method affects the band alignment: The post-growth transfer of TMD layers from a growth substrate (SiO_2/Si or sapphire) to the target SiO_2/Si wafer [13, 14] has been found to cause a ≈0.5–1eV VB shift ascribed to violation of the MoS_2/SiO_2 interface electroneutrality [15]. This transfer process becomes unavoidable when implementing MoS_2 and WS_2 in the IC production process because of the high growth temperatures (>800 °C in the presence of H_2S) needed to obtain a larger grain size and less grain boundaries [16–18] severely degrade insulating properties of SiO_2 [19]. At the same time, the band alignment represents a crucial factor directly influencing the built-in electric fields and the electron tunnelling rate across the interface and its knowledge and tight control are needed to ensure reproducibility of the devices.

In this work we addressed the critical issue of stability of 1 ML WS_2 films grown by metal-organic CVD (MOCVD) on SiO_2 as affected by storage in air and by layer transfer from the growth sapphire substrate to the device-relevant SiO_2/Si wafers. As in the earlier studies [11, 12, 15] we used internal photoemission of electrons

(IPE) from the VB of the TMD film into the SiO_2 conduction band (CB) to monitor evolution of the band alignment. In addition to the good reproducibility of the VB top energy position of 1ML WS_2 films directly grown on SiO_2/Si substrates we found that storage in air over extended period of time (up to 9-14 months) has no significant effect on the density of states in the TMD VB and their energy distribution. This result is significantly different from the previously reported instability of the 2- and 4-ML WS_2 films synthesized by annealing (sulfurization) of metallic W layers in H_2S [20]. Furthermore, contrary to the MoS_2 case [15], the band alignment of MOCVD-grown 1ML WS_2 is not significantly impacted by layer transfer processing. Taken together, these results indicate MOCVD-grown WS_2 as a superior candidate for wafer-scale device fabrication.

2. Experimental details

The 1 ML-thin WS_2 films were grown from $W(CO)_6$ and H_2S precursors using similar approach as previously used for the MoS_2 synthesis [10] on top of a-SiO_2(50nm)/p-Si(100) 300 mm wafers. Two sets of samples were fabricated under a different base pressure of the MOCVD reactor: A high one, with possible presence of oxygen (referred to as sample set 1) and the lower one, supposed to be 'purer' (sample set 2). To investigate the possible impact of the TMD layer transfer on the band alignment, two additional 1 ML WS_2 films were grown on top of sapphire wafers, using the same MOCVD approach as set 1 and subsequently transferred on top of identical a-SiO_2(50 nm)/Si substrates. One WS_2 film was transferred using the widely used technique of water intercalation-based Poly(methyl methacrylate) (PMMA) assisted transfer [15, 21] (the 'wet transfer' process). The other WS_2 film was first covered by a temporary adhesive/laser release layer on a glass carrier, then de-bonded from the growth wafer and permanently bonded in vacuum to the target a-SiO_2(50 nm)/Si wafer; after which the temporary glass stack was released by laser heating [22, 23] (the 'dry transfer' process).

On top all WS_2 films a combination of optically non-transparent small area contact pads (100 nm thick, 0.01 mm^2) and large area semi-transparent electrodes (15 nm thick, 0.5 mm^2) of Al, Au, and Cu were thermoresistively evaporated to minimize possible damage to the ML-thin films [24, 25]. A photograph of a sample from set 1 with Al and Au contacts can be found in figure 1(a). A blanket Al layer was used as the backside contact to the Si substrate wafer. IPE measurements were carried out at room temperature using a 150 W xenon arc lamp as light source in combination with a monochromator (spectral resolution of 2 nm) providing photons in the energy $h\nu$ range from 2 to 6 eV. In the biased 1 ML $WS_2/SiO_2/Si$ capacitors (schematic cross section is shown in figure 1(b)), currents were measured under illumination and in darkness using a Keithley 6517a electrometer. Then the photocurrent was calculated as the difference between these currents and, by normalizing the photocurrent to the calibrated incident photon flux of the xenon lamp at given $h\nu$, the quantum yield Y($h\nu$) was determined. To minimize transient effects a time delay between the start of illumination and the current readout was implemented, in combination with extensive averaging (>60 per current readout) in order to improve the signal-to-noise ratio. Powell's model [26] was used to analyse spectral dependencies of the quantum yield. In order to determine the IPE spectral threshold energy Φ_e, the quantum yield in the region above Φ_e can be approximated as a power function of the photon energy $h\nu$ [26]:

$$Y(h\nu) = A(h\nu)(h\nu - \Phi_e)^p, \quad (1)$$

where A($h\nu$) depends on the optical properties of the illuminated sample, including the possible optical interference effects and variations of optical properties of the constituent materials. It is usually assumed that this constant does not vary significantly within the narrow spectral range above the spectral threshold since no abrupt variations of the optical behaviour is expected [26]. The exponent p is determined by the emitter type, in this case electrons are emitted from the VB of WS_2 into the CB of SiO_2 and p is expected to be equal to 3, corresponding to a linear increase of the states with energy below the VB top edge [26]. Indeed, this linear increase has been directly observed in x-ray photoelectron spectroscopy VB spectra of 1ML WS_2 within approximately 1 eV range below the VB top [27]. Therefore, the IPE spectral threshold energy Φ_e corresponding to the minimal energy required for an electron to be excited from the WS_2 VB top edge into the CB of the underlying SiO_2 insulator can be found by linear fitting the quantum yield spectral curve in $Y^{1/3} - h\nu$ coordinates, also known as Powell coordinates. Finally, to account for the image-force barrier lowering effect [26], spectral thresholds determined at various externally applied gate bias voltages V_g are plotted in $\Phi_e - \sqrt{F}$ coordinates (the Schottky plot). These are then linearly extrapolated to a zero electric field F, determined by normalizing the V_g to the oxide thickness, to obtain the interface barrier height [24]. The built-in potential value related to the effective work function difference between Si and top electrode and possible presence of oxide charges was estimated from the voltage onset of the IPE current from WS_2 and subtracted from V_g.

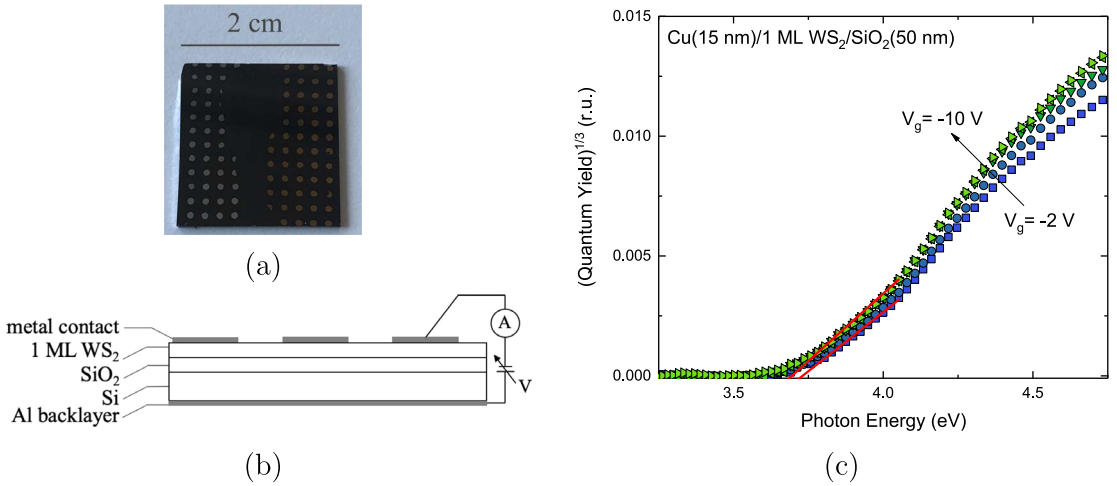

Figure 1. (a) Photograph of a sample from set 1 with semi-transparent Al (left) and Au (right) contacts (b) Schematic cross section of the measurement setup (c) Powell plot of the IPE quantum yield spectra of MOCVD-grown 1 ML WS_2 (sample set 1) with a semi-transparent Cu contact electrode as measured for Cu/WS_2 electrode bias voltages ranging from −2 V to −10 V. Red lines illustrate the linear fit used to determine the field dependent IPE thresholds.

3. Results

The IPE spectra from 1 ML WS_2 directly grown on SiO_2 can serve as a reference in order to trace the possible influences of the processing factors, e.g., the type of layer transfer, on band alignment at the WS_2/SiO_2 interface. Figure 1 shows an example of IPE spectra (in Powell coordinates) for a sample from the set 1 using semi-transparent Cu contacts to WS_2. It has already been established that electrons photoexcited inside the top metal layer provide an insignificant contribution to the photocurrent [12], i.e. the observed spectra are due to electron photoexcitation within the WS_2 layer. The (quantum yield)$^{1/3}$ of the IPE from WS_2 is seen to increase linearly with photon energy above $h\nu \approx 3.5$ eV allowing for the extraction of field dependent thresholds through linear fitting. The Schottky plot shown in figure 2 exhibits the IPE thresholds values obtained at different fields as well as the thresholds inferred from IPE measurements at 2 different locations within the wafer using a non-transparent Al contact. The results of two different contact schemes/contact metals are perfectly consistent yielding, by linear extrapolation of thresholds to a zero electric field, the zero field threshold of 3.7 ± 0.1 eV corresponding to the energy barrier between the 1 ML WS_2 VB top and the SiO_2 CB bottom edge. The same threshold values obtained from different places within the growth wafer indicate good homogeneity of the MOCVD deposited WS_2 in terms of the VB top energy.

To further examine the reproducibility of the MOCVD growth, IPE measurements were carried out on sample set 2 of 1 ML WS_2 also directly grown on SiO_2. Figure 3 compares two spectra of this particular sample with Al semi- and non-transparent contacts to the spectrum of sample set 1. Spectra measured with non-transparent contact pads are normalized to match the spectra with semi-transparent contacts because the illuminated area of WS_2 photoemitter is expected to be smaller for the former case. This normalization is performed by aligning the maximum quantum yield for IPE from the Si backside photoemitter, used as the reference, at a + 5 V gate bias. In the relevant spectral range ≈1 eV above Φ_e the IPE spectra for sample set 2 are practically identical to those observed in sample set 1 indicating good reproducibility of the used MOCVD process. However, as the sample set 1 was grown at a higher base pressure suggesting a small air leak, presence of oxygen and nitrogen during WS_2 synthesis is expected. Nevertheless, the observed reproducibility of IPE spectra within the 1 eV region above the spectral threshold indicates that the presence of oxygen and nitrogen is not significantly impairing the band structure of the WS_2/SiO_2 interface for the H_2S pressure used (see Ref. [10] for details). Thus, the applied MOCVD process appears to be sufficiently "tolerant" to a limited presence of oxygen and nitrogen, with insignificant variations in the band structures below the valence band top edge. We suggest that, in the H_2S reactive ambient, W oxides and nitrides are converted into the desirable WS_2 compound resulting in a kind of 'self-cleaning' process during layer synthesis. For example, thermal sulfurization in H_2S at 900 °C is shown to convert MoO_x and WO_x layers deposited from nitrogen-containing precursors into stoichiometric MoS_2 and WS_2, respectively [28].

Additionally, the origin of the 'diverging' spectral curves at $h\nu > 4.5$ eV for the sample from batch 2 can be found in the aluminium contact, as the spectral curves are measured on the same chip with the thickness of top Al contact (100 or 15 nm) being the only physical difference. The optical excitation of electrons at the top

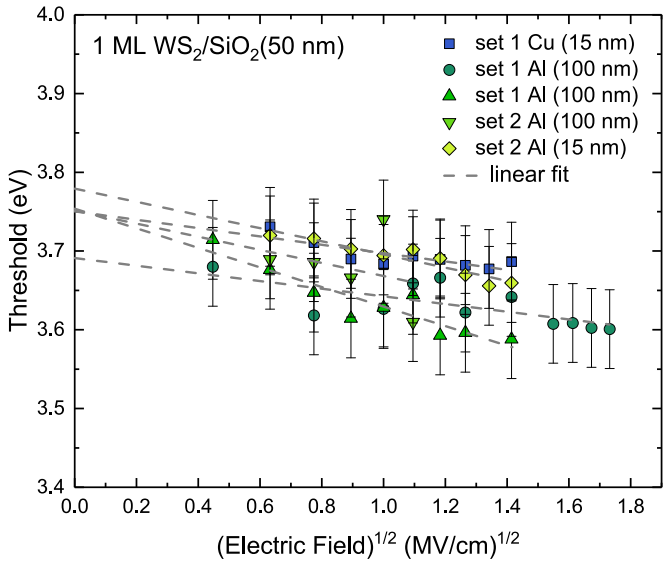

Figure 2. Schottky plot of the inferred IPE threshold values for both sets of 1 ML MOCVD WS_2 samples for different metal contacts. The grey dashed lines illustrate the linear fit used to obtain the zero field threshold.

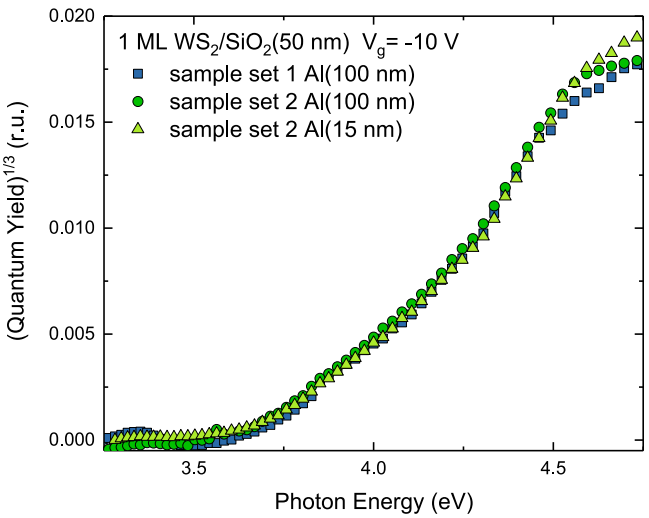

Figure 3. Comparison (in the Powell coordinates) between IPE spectral curves measured on samples from the different growth sets of the 1 ML MOCVD WS_2 films for the same gate bias voltage of −10 V. The IPE spectra are normalized using IPE current from the opposite Si substrate electrode in order to account for the differences in the illuminated WS_2 area.

Al/WS_2 interface in the sample with thin semitransparent Al electrode represents the most probable source of the additional IPE current observed in this sample at $h\nu > 4.5$ eV as opposed to the case of non-transparent 100 nm thick electrode. This hypothesis is supported by the fact that, if plotted in the Fowler coordinates ($Y^{1/2} - h\nu$), the 'extra' yield has spectral threshold of 4.2–4.3 eV which is close to the work function of metallic Al [29]. If not coincidental, this observation suggests that electron IPE from Al into SiO_2 across 2D material WS_2 becomes possible when the energy of electrons becomes sufficient to be ballistically transported across the Van der Waals (vacuum) gap. For comparison, electron IPE from Al evaporated directly on SiO_2 has a spectral threshold (at zero field) of 3.2–3.3 eV [30].

The good reproducibility of the MOCVD process is further supported by the results shown in the Schottky plot (figure 2), where the extracted field dependent thresholds of set 2 are presented for comparison with linear extrapolation yielding the same zero field barrier of 3.7 ± 0.1 eV. Therefore, we may conclude that the VB top edge of the MOCVD-grown 1 ML WS_2 is reproducibly found at 3.7 eV below the CB bottom edge of SiO_2 irrespectively of the used contacting scheme. The impact of different metals (Al, Cu, Au) used as a contact pad on the WS_2/SiO_2 interface band alignment has been previously explored [12]. These results show marginal sensitivity of the VB top position in WS_2 to the contact metal indicating that electron IPE predominantly occurs from the un-metallized WS_2 area surrounding the contact pad. Furthermore, the results of this present work

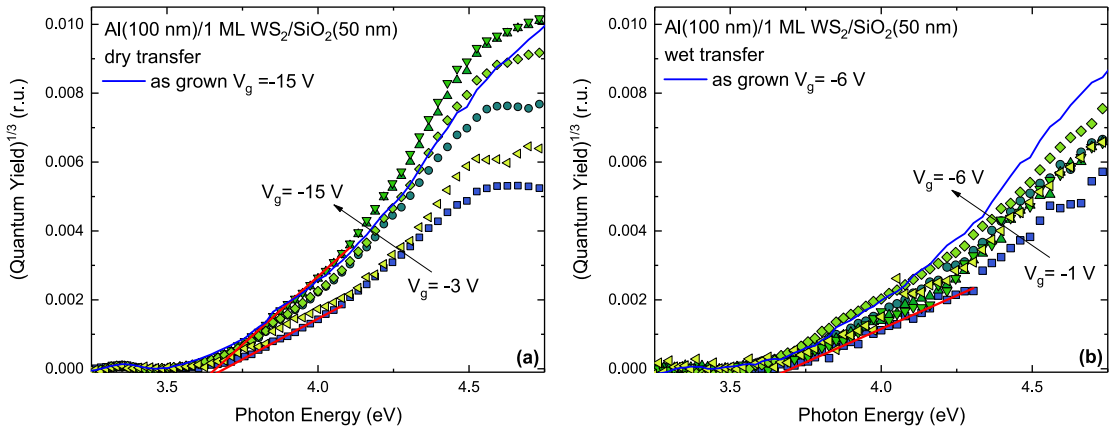

Figure 4. Powell plot of the IPE quantum yield spectra of MOCVD-grown 1 ML WS_2/SiO_2 samples with a non-transparent Al contact pad for (a) WS_2 transferred using the dry transfer process for gate bias voltages ranging from −3 V to −15 V. (b) WS_2 transferred using the wet transfer process for gate bias voltages ranging from −1 V to −6 V. Red lines illustrate the linear fit used to obtain the field dependent IPE threshold. As a comparison in both figures an IPE spectral curve of as grown material is plotted at the highest measured applied gate bias.

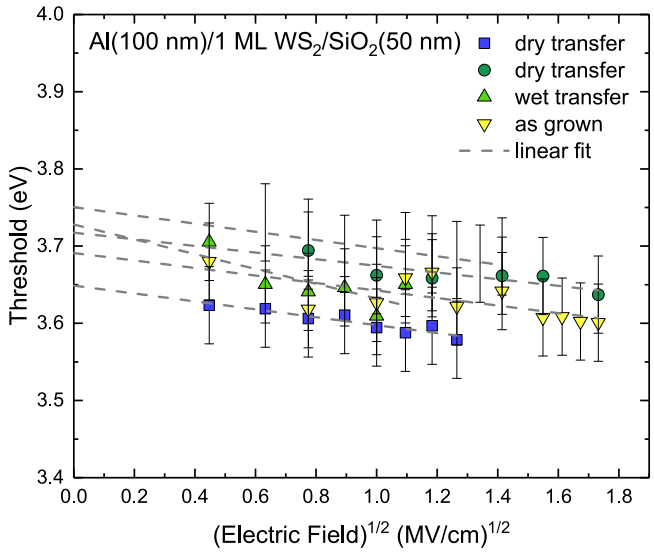

Figure 5. The Schottky plot of the IPE electron threshold values for as grown and transferred (dry or wet) 1 ML WS_2. Dashed lines indicate the linear fit used to obtain the zero field threshold value.

reveal that even in the case of electron IPE from the WS_2 covered by a continuous layer of semi-transparent Al (15 nm thick) the spectral threshold remains unchanged (cf figure 3). This suggests that the used gentle thermoresistive evaporation of metal contacts leaves electron states in WS_2 intact. Furthermore, the field dependence of thresholds in figure 2 does not change significantly between different samples indicating similar electrostatics of the WS_2/SiO_2 interface. These consistent results regarding band alignment at the WS_2/SiO_2 interface can now be used as a benchmark to evaluate the possible transfer-induced changes to the band alignment or the effects of the sample storage.

First we addressed the samples prepared using the dry transfer method as this minimizes the WS_2/SiO_2 interface exposure to water which was seen as the primary suspect responsible for the formation of interface dipoles and charges [15]. Figure 4(a) shows the typical IPE spectra of dry transferred MOCVD-grown 1ML WS_2 which appears to be surprisingly similar to those observed for the directly-grown 1 ML WS_2 (cf figure 1) suggesting that the transfer process has no significant impact on the IPE. Both the transferred and directly grown samples have similar maximum quantum yield values indicating that the photoexcited volume of WS_2 is barely affected by the transfer. The inferred field dependent thresholds are compiled in the Schottky plot (figure 5) together with the thresholds obtained from a different contact pad (original spectra not shown). Linear extrapolation to zero electric field yields the barrier height of 3.7 ± 0.1 eV, i.e. exactly the same as the value found for the WS_2 directly grown on SiO_2. Furthermore, the field dependence of the IPE thresholds remains essentially

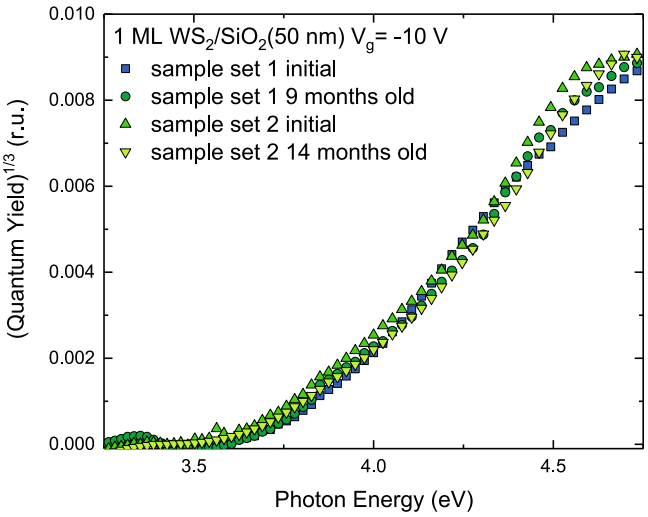

Figure 6. Powell plot of the IPE quantum yield spectra of two sets of MOCVD-grown 1 ML WS_2 measured during two storage periods for a bias gate voltage of −10 V. Initial measurements were performed closely after growth with subsequent measurements in between with the final measurements performed approximately 9 and 14 months for set 1 and 2, respectively after the initial IPE experiment.

unchanged indicating an insignificant variation of the interface electrostatics, i.e. the absence of additional electric fields. These results indicate the stability of the band alignment after 2D layer transfer through the dry transfer process.

Next, it is still worth examining the widely adopted wet transfer method. Figure 4(b) shows IPE spectra for 1 ML WS_2 after wet transfer onto SiO_2 which exhibit behaviour similar to that observed for the already discussed directly grown layers. A somewhat reduced maximum quantum yield does not imply a large change in photoexcited WS_2 volume and might be related to the slight barrier transparency change. Obviously, there are no effects observed in the case of sulfurization-grown MoS_2 layers transferred onto SiO_2 [15]. The inferred field dependent thresholds are compiled in the Schottky plot (figure 5) with linear extrapolation resulting in the same value of the zero field threshold of 3.7 ± 0.1eV as in the directly-grown WS_2/SiO_2 entities. As compared to the dry transferred WS_2 layers there is a small change in threshold field dependence slope which, however, falls within the range of variations observed in the case of directly grown films (figure 2). Furthermore, this field dependence change is marginal when compared to the field dependent IPE threshold changes observed for the transferred 2 ML MoS_2 using the same wet transfer process [15]. Thus, the MOCVD-grown 1ML WS_2 appears to be by far more stable (than MoS_2) in terms of the electronic structure, the band alignment at the interface with underlying SiO_2, and the electrostatics of this interface after been subjected to the critically important technological step of the layer transfer (both wet and dry). These results combined with the improved characteristics of electron transport make WS_2 a more attractive candidate for the device implementation on a wafer scale than MoS_2.

Finally, based on the revealed reproducibility of the MOCVD WS_2 growth process, we addressed the resistance of these MLs against oxidation in air because the previous study conducted on the sulfurization-grown WS_2 films revealed their inferior stability as compared to MoS_2 films synthesized in the same way [20, 25]. In general, the thin 2D TMD layers are well known to suffer from oxidation in air leading to significant degradation of their electronic properties [31–33]. In particular, CVD-grown WS_2 films have been found to show signs of oxidation within mere days/months [34] or a year [31] of storage. Therefore, we repeated the IPE spectral measurements on samples stored in ambient conditions which could reveal signs of film degradation. The WS_2 films investigated here were stored in room ambient, i.e. without any drying desiccant, which has been found to worsen the effect of oxidation [31]. Figure 6 shows a comparison of the IPE spectra of both sets of MOCVD 1ML WS_2 directly synthesized on top of SiO_2; the initial measurements were conducted right after the growth and metallization processing (<1 day) while the final measurements were performed 9–14 months after film synthesis. Would any significant oxidation of the film occur the IPE quantum yield would be reduced and accompanied by a shift of the IPE energy onset towards higher photon energies as observed for 2 ML WS_2 grown through sulfurization of metallic tungsten [20, 25]. However, no such shift is observed (figure 6), both the initial and the 'aged' sample spectra are essentially identical within ≈1eV wide spectral range above photoemission threshold. Furthermore, the maximum quantum yield values remain comparable in both cases indicating an insignificant change in photoexcited volume which would indicate 'disappearance' of WS_2 due to formation of the oxygen-containing bonds. These results suggest that the studied MOCVD-grown WS_2

films are sufficiently resistant to air exposure in order to allow one to process them under conventional clean-room conditions.

The available results on oxidation of WS_2 and MoS_2 under ambient conditions indicate that the initial oxygen reactions occur at the edges of 2D islands and grain boundaries suggesting crucial role of defects in the oxidation chemistry. A similar conclusion can be made on the basis of oxide nucleation analysis during atomic layer deposition of oxide overlayers on top of 2D TMD semiconductors. In this spirit, the possible explanation for the increased resistance of this MOCVD grown material to air exposure compared to the sulfurization grown WS_2 could be the difference in the structure of point defects. In the case of similarly grown MoS_2 layers, i.e. metal sulfurization in H_2S versus MOCVD from $Mo(CO)_6$ and H_2S at the same temperatures as used in the present work, electron spin resonance (ESR) measurements revealed structurally different defects: Sulfur vacancies are the most abundant defects in MoS_2 grown through sulfurization of metallic Mo [35]; such defects are known to accelerate oxidation [36]. By contrast, ESR measurements on MoS_2 layers grown by similar MOCVD process as used here for the WS_2 samples reveal Mo vacancies as the dominant defect [18]. As both the investigated MoS_2 and WS_2 were grown according to the same procedure in the same reactors one may expect the defects to be the same in both Mo and W disulfides. This suggestion is supported by ESR observation of signal closely resembling LM1 signal in MoS_2 (see Ref. [7]) in the similarly sulfurization-grown 2ML thick WS_2 [37]. This difference in the nature of the growth-induced defects will obviously affect chemical reactivity of the surfaces and might explain the increased stability against oxidation of MOCVD grown WS_2.

4. Conclusion

In conclusion, using internal photoemission spectroscopy we demonstrated that the MOCVD-grown 1 ML WS_2 films are sufficiently robust to withstand two most important technological factors critical for their implementation in the wafer-scale semiconductor processing. First, in sharp contrast to MoS_2, transfer (both 'dry' and 'wet') has no significant impact the band alignment at the 1 ML WS_2/SiO_2 interface with no indications of interface charges/dipoles introduced in the barrier region. Second, the MOCVD-grown 1 ML WS_2 films appear to be remarkably resistant against oxidation in air promising great simplification in their post-synthesis handling. Summarizing these findings, we conclude that MOCVD-grown WS_2 represents the 'processing-friendly' material with good potential for practical implementation in the IC technology.

Acknowledgments

This work was financially supported by the Flanders Innovation & Entrepreneurship [2Dfun (2D functional MX_2/graphene heterostructures), an ERA-NET project in the framework of the EU Graphene Flagship] and by a KU Leuven Internal Fund (project C14/16/061).

Data statement availabiliy

The data that support the findings of this study are available upon reasonable request from the authors.

ORCID iDs

G Delie https://orcid.org/0000-0002-5646-3261
C Huyghebaert https://orcid.org/0000-0001-6043-7130
V V Afanas'ev https://orcid.org/0000-0001-5018-4539

References

[1] Radisavljevic B, Radenovic A, Brivio J, Giacometti V and Kis A 2011 *Nat. Nanotechnol.* **6** 147–50
[2] Wang H, Yu L, Lee Y H, Shi Y, Hsu A, Chin M L, Li L J, Dubey M, Kong J and Palacios T 2012 *Nano Lett.* **12** 4674–80
[3] Wang J *et al* 2016 *Adv. Mater.* **28** 8302–8
[4] Liu H, Neal A T and Ye P D 2012 *ACS Nano* **6** 8563–9
[5] Rawat A *et al* 2018 *J. Mater. Chem.* A **6** 8693–704
[6] Georgiou T *et al* 2013 *Nat. Nanotechnol.* **8** 100
[7] Chiappe D *et al* 2016 *Advanced Materials Interfaces* **3** 1500635
[8] Freedy K M, Litwin P M and McDonnell S J 2017 *ECS Trans.* **77** 11
[9] Ling Z *et al* 2015 *Opt. Express* **23** 13580–6
[10] Chiappe D *et al* 2018 *Nanotechnology* **29** 425602
[11] Shlyakhov I, Chai J, Yang M, Wang S, Afanas'ev V, Houssa M and Stesmans A 2018 *APL Mater.* **6** 026801

[12] Delie G, Litwin P M, McDonnell S J, Chiappe D, Houssa M and Afanas'ev V V 2020 *ECS Journal of Solid State Science and Technology* **9** 093009
[13] Elías A L *et al* 2013 *ACS Nano* **7** 5235–42
[14] Xu Z Q *et al* 2015 *ACS Nano* **9** 6178–87
[15] Afanas'ev V, Chiappe D, Perucchini M, Houssa M, Huyghebaert C, Radu I and Stesmans A 2018 *Nanotechnology* **30** 055702
[16] Asselberghs I *et al* 2020 Scaled transistors with 2D materials from the 300 mm fab *2020 IEEE Silicon Nanoelectronics Workshop (SNW) (IEEE)* pp 67–8
[17] Stesmans A, Iacovo S, Chiappe D, Radu I, Huyghebaert C, De Gendt S and Afanas'ev V 2017 *Nanoscale Res. Lett.* **12** 1–5
[18] Schoenaers B *et al* 2020 *ECS Journal of Solid State Science and Technology* **9** 093001
[19] Stesmans A and Afanas'ev V 1996 *Appl. Phys. Lett.* **69** 2056–8
[20] Afanas'ev V V, Chiappe D, Leonhardt A, Houssa M, Huyghebaert C, Radu I and Stesmans A 2017 *ECS Trans.* **80** 191
[21] Chiappe D 2016 Molybdenum disulfide film formation and transfer to a substrate *US Patent Specification* 9,472,401
[22] Huyghebaert C *et al* 2018 2D materials: roadmap to cmos integration *2018 IEEE International Electron Devices Meeting (IEDM) (IEEE)* (https://doi.org/10.1109/IEDM.2018.8614679)
[23] Phommahaxay A *et al* 2019 The growing application field of laser debonding: From advanced packaging to future nanoelectronics *2019 International Wafer Level Packaging Conference (IWLPC) (IEEE)* pp 1–8
[24] Afanas'ev V, Chiappe D, Huyghebaert C, Radu I, De Gendt S, Houssa M and Stesmans A 2015 *Microelectron. Eng.* **147** 294–7
[25] Afanas'ev V *et al* 2020 *J. Phys. Condens. Matter* **32** 413002
[26] Powell R 1970 *J. Appl. Phys.* **41** 2424–32
[27] Zhu H *et al* 2018 *Appl. Phys. Lett.* **112** 171604
[28] Sharma A, Mahlouji R, Wu L, Verheijen M A, Vandalon V, Balasubramanyam S, Hofmann J P, Kessels W E and Bol A A 2020 *Nanotechnology* **31** 255603
[29] Derry G N, Kern M E and Worth E H 2015 *Journal of Vacuum Science & Technology A: Vacuum, Surfaces, and Films* **33** 060801
[30] Solomon P and DiMaria D 1981 *J. Appl. Phys.* **52** 5867–9
[31] Gao J, Li B, Tan J, Chow P, Lu T M and Koratkar N 2016 *ACS Nano* **10** 2628–35
[32] Zhang Y *et al* 2013 *ACS Nano* **7** 8963–71
[33] Ly T H *et al* 2014 *ACS Nano* **8** 11401–8
[34] Kotsakidis J C, Zhang Q, Vazquez de Parga A L, Currie M, Helmerson K, Gaskill D K and Fuhrer M S 2019 *Nano Lett.* **19** 5205–15
[35] Houssa M, Iordanidou K, Pourtois G, Afanas'ev V and Stesmans A 2017 *Appl. Surf. Sci.* **416** 853–7
[36] Kc S, Longo R C, Wallace R M and Cho K 2015 *J. Appl. Phys.* **117** 135301
[37] Stesmans A 2019 Private communication